

6th Asia Pacific Workshop on Structural Health Monitoring, 6th APWSHM

## An investigation of the use of embedded FBG sensors to measure temperature and strain inside a concrete beam during the curing period and strain measurements under operational loading

C Fernando <sup>1</sup>, A. Bernier <sup>2</sup>, S Banerjee <sup>4</sup>, G Kahandawa <sup>5</sup>, J Eppaarchchi <sup>3</sup>

<sup>1</sup> University of Southern Queensland, Health Engineering and Surveying, QLD4350, Australia.

<sup>2</sup> Federation University School of Engineering and Information Technology, Gippsland, VIC3842, Australia.

Email: G.Fernando@usq.edu.au; Jayantha.Epaarachchi@usq.edu.au

### Abstract

This paper covers detailed investigation on the use of a FBG sensor for temperature and strain measurement in a reinforced concrete beam within first 28 days after pouring and structural response after 28 days curing period. A Fiber Bragg grating (FBG) sensor and a few thermo-couples (TC) have been embedded in the concrete beam at the casting stage. After curing the beam was laterally loaded on a three-point bending arrangement until a crack formed on the beam and subsequently heated to 200 °C with a 5kN lateral load at mid-span. A detailed analysis was performed on the data obtained from FBG sensor, thermo-couples and surface mounted electrical strain gauges (SG). Further, the cracked surface was continuously monitored with an Infrared Red (IR) camera during the heating to establish the temperature profile of the cracked surface of the concrete beam. A detailed Finite Element Analysis (FEA) of the concrete beam (structural and thermal) was performed using ABAQUS and compared with the experimental results.

© 2016 The Authors. Published by Elsevier Ltd. This is an open access article under the CC BY-NC-ND license (<http://creativecommons.org/licenses/by-nc-nd/4.0/>).

Peer-review under responsibility of the organizing committee of the 6th APWSHM

Temperature; Strain; Concrete Structures.

### 1. Introduction

Infrastructure systems are critical for sustaining and maintaining a nation's socioeconomic system. The critical infrastructure is a term used by governments to describe assets that are essential for the functioning of a society and economy. The critical infrastructure systems are complex systems that are dynamic. During a typical lifespan, critical infrastructure is inevitably subjected to environmental effects, long-term loading effects, material deterioration and/or extreme loading effects such as corrosion, fatigue, aging, earthquakes, hurricanes, extreme temperature, etc. The increased use of critical infrastructure for load bearing structures has alarmed the related industries to immediate need of structural health monitoring (SHM) systems to ensure safe operation of the critical infrastructure. The SHM process is an important feature to achieve technological leaps in the design and operation of engineering infrastructures. Karbhari (2005) stated a generalized definition of SHM featuring non-destructive in-situ sensing. The SHM process involves analysis of structural characteristics and structural response for the purpose of estimating the severity of damage / deterioration. Then SHM evaluates the consequences thereof on the structure in terms of response, capacity and service life. Karbhari and Ansari (2009) described that a SHM system includes main operations of acquisition, validation, analysis, prognosis and management. In SHM miniaturized sensors have been embedded in smart composite materials in order to mitigate the risk of failure due to an overload or an unwanted inhomogeneity resulting from the fabrication process (Kinet et al 2014). Monitoring strain by measuring the wavelength shift of the light reflected from the FBG sensor has often been applied in conventional health monitoring. Epaarachchi et al. (2007, 2009), Kahandawa et al (2011) have successfully used embedded FBG sensors to measure internal strain and investigated the change of spectral shapes and change of strain in the vicinity of a damage. FBG sensors have attracted much attention for SHM applications due to their great advantages, such as high accuracy in measuring strain and/or temperature and multiplexing capability (Hill and Meltz 1997; Kersey et al. 1997).

### 2. SHM in Concrete Structures

Reinforced concrete structures are commonly exposed to thermal loads as a result of the design function of the structure, ambient conditions, heat of hydration, exposure to fire, etc. Thermal loads can give rise to significant levels of stress, distortion, and damage as a consequence of nonlinear temperature and strain profiles (producing primary thermal stresses) and restrained structural deformation (producing secondary or continuity thermal stresses) (Priestley, 1981). The small diameter FBG sensors (diameter less than 250 micrometers) will not affect the structural integrity and enables fast interrogation (Herszberg et al. 2008). Damage diagnosis systems is the basis of an effective strain based SHM system. This system generally consists of damage detection, identifying the location and extent of the damage and not essentially but desirably the cause of the damage. FBG sensors are

operated by creating variations in the refractive index of the core of an optical fiber (Meltz et al. 1989). FBG sensors are fabricated in the core region of specially fabricated single mode low-loss germanium doped silicate optical fibers. The grating is the laser-inscribed region which has a periodically varying refractive index. This region reflects only a narrow band of light corresponding to the Bragg wavelength  $\lambda_B$ , which is related to the grating period  $\Lambda_0$  (Kashyap 1999).

$$\lambda_B = \frac{2n_o \Lambda_0}{k} \tag{1}$$

Where  $k$  is the order of the grating and  $n_o$  is the initial refractive index of the core material prior to any applied strain.

Due to the applied strain,  $\epsilon$ , there is a change in the wavelength,  $\Delta\lambda_B$ , for the isothermal condition,

$$\frac{\Delta\lambda_B}{\lambda_B} = \epsilon P_e \tag{2}$$

Where  $P_e$  is the strain optic coefficient and calculated as 0.793.

$$\Delta\lambda_B = \lambda_B \{ (\alpha + \epsilon) \Delta T + (1 - p_e) \Delta \epsilon \} \tag{3}$$

Su and Han, 2014 discovered that the bragg wavelength varies linearly with strain and/or temperature. The amount of strain and/or temperature change present determines the degree of external disturbance and thus the amount of grating period and Bragg wavelength variance. The variation of the Bragg wavelength can be obtained by above equation where  $\Delta\epsilon$  is the strain variation,  $\Delta T$  is the temperature change,  $\alpha$  is the coefficient of the thermal expansion,  $\epsilon$  is the thermos optic coefficient,  $P_e$  and is the strain-optic coefficient.

**3. Experimentation**

A high strength Grade 40 MPa concrete was used to pour two identical concrete beams with the dimension of 100mm X 250 mm X 1400 mm as seen in figure 1 a and 1 b. FBG sensors and thermocouples have been embedded to the structure during casting to check the ability of FBG sensors to measure strain and the temperature variation of the concrete beam. The variation of the temperate was monitored during 28 days after casting and beyond. After 28 days of pouring the concrete, one beam was loaded laterally in a three-point bending arrangement until a cracked was formed.

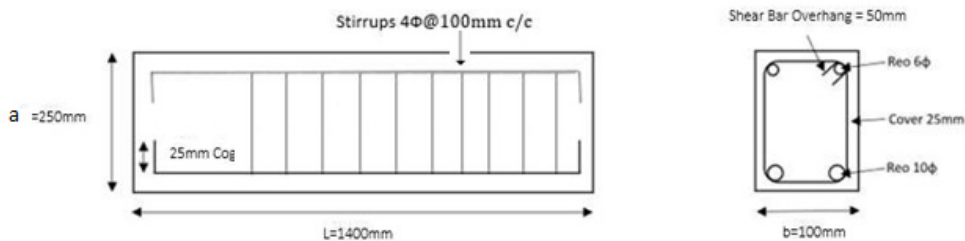


Fig 1 a

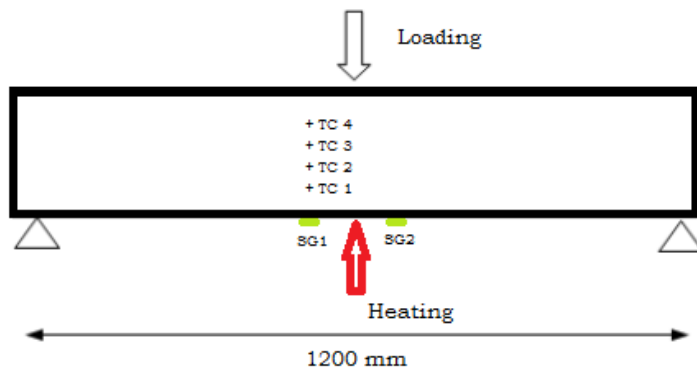


Fig 1 b

Fig 1 a- Schematic view of the concrete prototype, b- sensors heating and loading setup.

A FEA method was used to determine the placement of the FBG sensors, thermocouples and electrical strain gauges. The concrete prototype model was created in a commercially available FEA software, ABAQUS. A FEA mesh was created and the model was stimulated in a three-point bending setup to study the stress levels of the beam. The linear elasticity, Young's modulus, Poisson's ratio  $\nu$  and coefficient of thermal expansion of the concrete, were directly fed into the FEA model.

As seen in figure 2, It can be seen that the FBG sensor needed to be placed at the z, y, z coordinates of 50, 60, 600 (millimetres from origin). The FBG sensors was placed parallel to strain axes in order to record maximum principal strains and to directly compare the theoretical strain from the FEA model. It is required to have an enclosure when embedding the FBG sensors. It is desirable that the design of the protective enclosure be critical to have efficient strain transfer from the main structure to the sensor with de-bonding from the main structure and the structural behaviour is not compromised with the sensor deployment (Biswas et al 2009). It is important to design a FBG enclosure that can be embedded into a concrete structure without degrading the strength of the concrete. FBG enclosures having the same material properties as the main concrete structure would minimise the damage that can create as result of embedding a foreign enclosure with different material properties. Figure 2 a and b display the FBG concrete enclosure that was designed and produced in order to reduce the loss of structural strength. 8mm diameter 80mm long plastic tube was used the mould. 40 MPa concrete mixture made and poured to the plastic beam. The FBG sensor was placed in the centre axis of the cylinder while pouring the concrete. After 10 hours of curing, the FBG concrete enclosure was removed from the mould and embedded inside the concrete beam during the casting.



Fig 2 a



Fig 2 b

Fig 2 a- Concrete FBG enclosure in the mould, 2-b FBG concrete enclosure

In order to validate the strain values recorded by the FBG sensor, two electrical strain gauges were to be surface mounted on the beams at the positions. It can be seen that the strain gauges (SG) were to be placed at the z, y, z coordinates 50,0, 600 and 50, 0, 800 (millimetres from axes). The strain gauges were to be placed longitudinally so that they could read maximum principal strains and be directly comparable to the FBG Sensor readings. The strain gauges were to be equally spaced from the centre of the beam. The surface of the beam where the strain gauges were to be mounted was first smoothed via the use of sand paper. Then a thin layer of quick set epoxy was smoothed onto the surfaces. After the epoxy had dried the strain gauges were glued to this surface via the use of the quick set epoxy followed by sticky tape. The strain reading of the electrical strain gauges will enable to calculate the theoretical strain levels of the structure in specific locations. These values were compared to validate that FBG strain reading. FBG reading was recorded using Micron optics SM125 Optical Spectrum Analyser(OSA).

In order to validate the temperature readings recorded with FBG sensor and provide an overall temperature profile of the beam, thermocouples were to be embedded in the beams at the positions shown in the figure 1-b and figure 3. Type J thermocouples have the ability to read high temperatures between the range of - 95 °C to 760 °C (degrees Celsius). The thermocouples were to be placed at the z, y, z coordinates 50,60, 600; 50, 105, 600; 50, 145, 600; and 50, 190, 600 (millimetres from origin) as identified by the FEA modelling. The thermocouples were calibrated with a known temperature before capturing the data. A NI cDAQ-9174 module and LABVIEW software were used to capture continuous temperature readings over a period of 28 days.

After 28 days of pouring the concrete, one beam was loaded laterally in a three-point bending arrangement. The prototype was loaded on the MTS 1000kN machine. The load levels were increased from 0 to 100 kN by 5kN steps until a cracked was formed as seen in figure 1 b (without heating). It was noted that a crack was formed at 61.68 kN. Then the cracked beam was heated with a 2 kilowatt heat source up to 200 °C and loaded with a 5kN load to in a three-point bending arrangement. The heat was applied on the side face of the beam within a concentrated 200-millimetre diameter circle. While heating the cracked surface was monitored through an IR camera continuously to observe the temperature profile. Most infrared cameras have the ability to compensate for different emissivity values, for different materials. In general, the higher the emissivity of an object, the easier it is to obtain an accurate temperature measurement with an infrared camera. Therefore, a thin layer of black paint was applied on the cracked surface in order to achieve a higher emissivity.

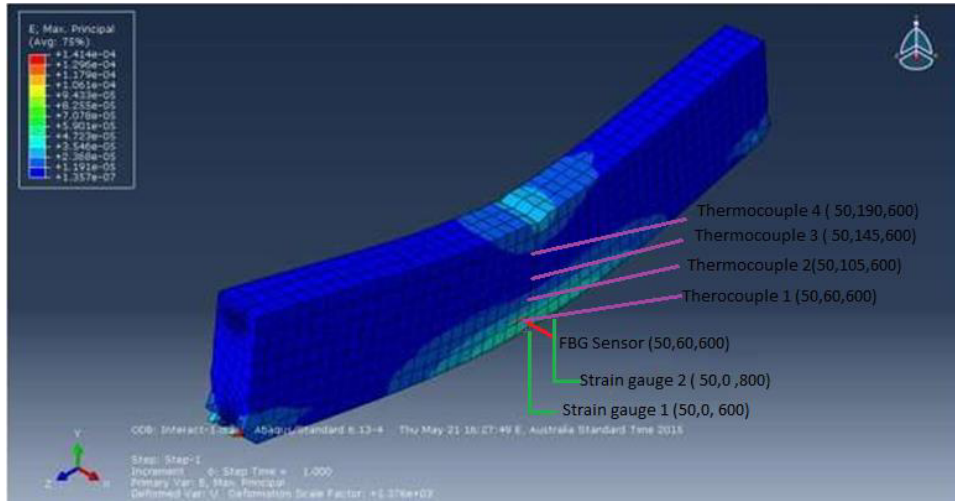


Fig3 – FEM Analysis of three-point bending arrangement.

4. Results and Discussion

It was observed that when the concrete cures, the temperature inside the concrete beam increases rapidly to reach a maximum after approximately 15 hours after pouring. From the below figure 4, it is suggested that the concrete beam specimens will show a rapid rise in internal temperature until it reaches a maximum temperature of approximately 23 °C, 15 hours after pouring. After this point the internal temperature of the concrete beam is declined until it reaches its approximate the ambient temperature, 30 hours after pouring. It can be seen that the temperature reading of the FBG sensors was slightly lower than the thermocouple reading TC1.

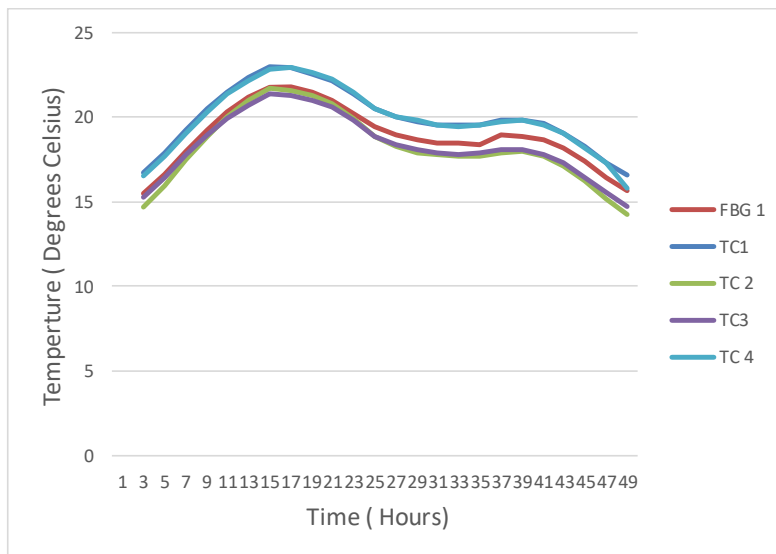


Fig 4 Temperature variation of the concrete beam during curing

Figure 5 shows the thermocouple readings and FBG temperature readings which were placed in the concrete beam as seen in figure 1-a when the beam was heated. It can be seen that the beam was subjected to a continuous heat for approximately one hour. After one hour beam reached a maximum temperature of approximately 148 °C. Then the beam took a five hours after reaching the maximum temperature to cool back down to ambient temperature.

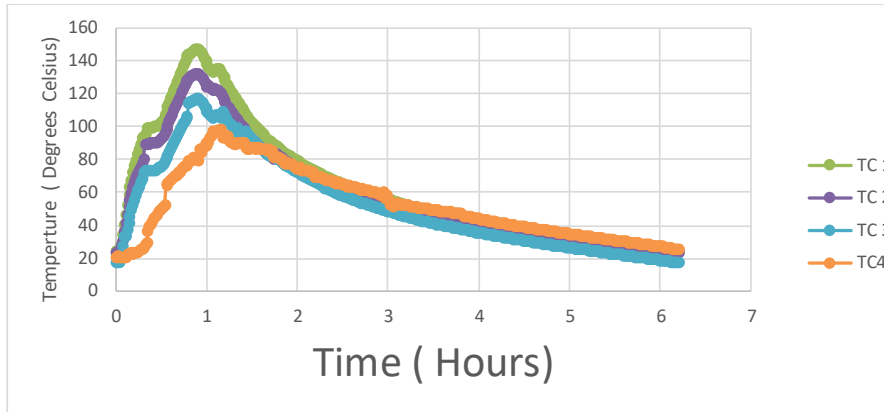


Fig 5 Temperature variation of the concrete beam during heating

The temperature data recorded in the FBG sensor and the thermocouple data of the same position were plotted as seen in Fig 6. It was noted that the FBG temperature reading is lower than the TC1 even though both sensors were placed on the same location. This is due to the fact that the FBG sensor data includes combination of temperature and the internal strains occurred during heating.

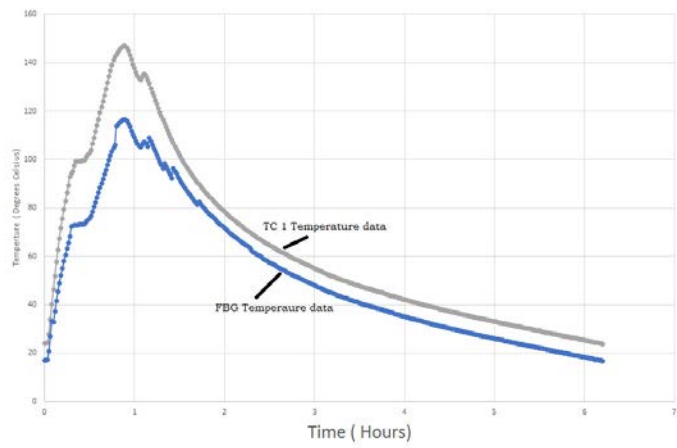


Fig 6 Temperature variation recorded with the FBG and the Thermocouple 1

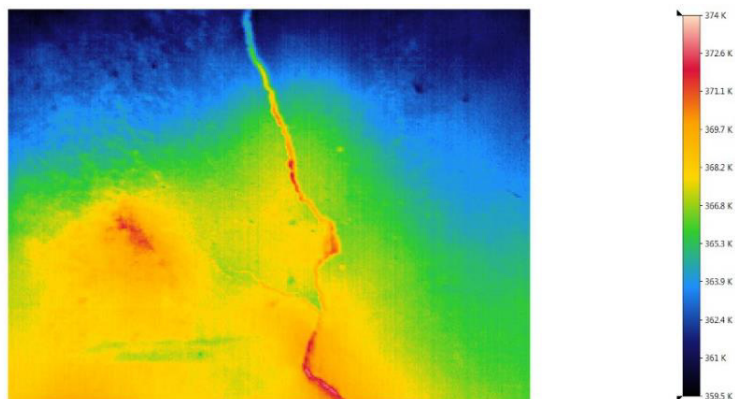


Fig 7. Thermography of the heated beam

As seen in the IR thermography picture Fig 7, the propagated crack is visible due to the the variation of temperature through crack due the presence of an air gap . Temperature near the heat source indicated a temperature 100.4 degrees Celsius ( 374 Kelvin) . A temperature of 85.85 degrees Celsius ( 359 Kelvin) was recorded at the crack.

Figure 8a shows the FBG sensor spectrum for both no load and 60kN loading conditions. The 60 kN load spectrum shows the strain concentrations caused by the crack in the concrete beam. In the spectrum of FBG has moved a little but the peak of the spectrum is intact. The observation of divided peaks of FBG sensors has been reported by several researchers in the vicinity of a damage Takeda et al 2008 the below. The FBG readings were in line with the theoretical calculation, electrical strain gauges and the FEA as seen in Fig 8 b, c, d.

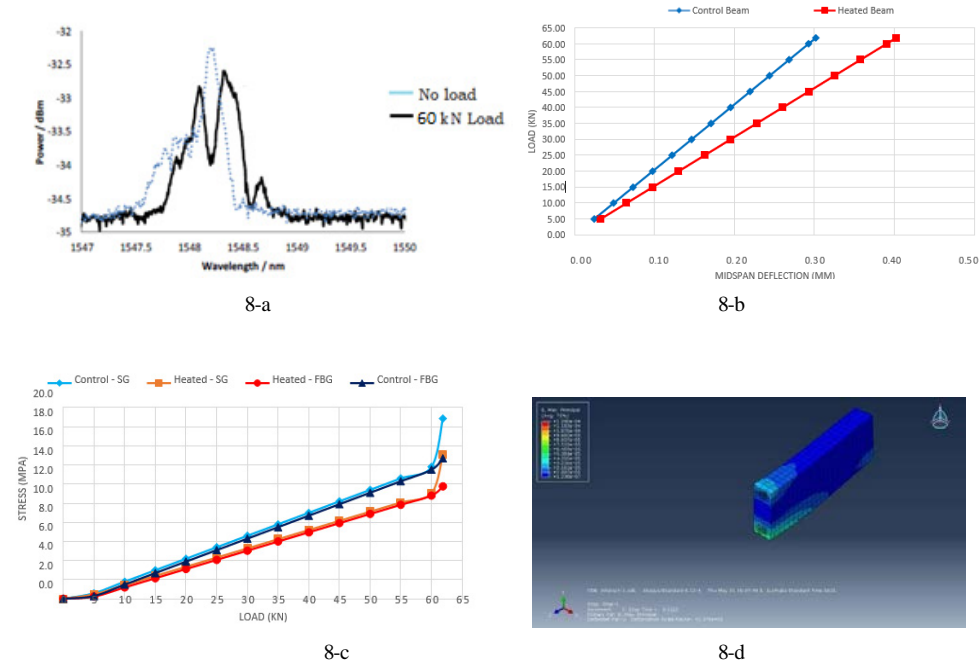


Fig 8 a- FBG Sensor Spectra, 8 b- Theoretical mid span deflection of the beam  
8 c Stress at various Loads of the beam, 8d FEA of the beam cross section

### 5. Conclusion

The FBG Sensors were proven to be capable of identifying internal deformations in concrete structures that cannot be seen via visual inspection. Use of concrete FBG enclosure when embedding the sensors allowed to place the sensor at a specific location easily. Also the use of concrete as the enclosure material made structure and the enclosure having same material composition and properties. An interruption in the FBG spectrum allows for the recognition of such deformations. These FBG sensors can also continuously real time monitor and record data relating to temperatures, strains, and vibrations. If a natural disaster occurs within an area, these sensors could allow for the determination of the extent a specific concrete structural elements are affected by such a disaster or just by long term use. IR technique of monitoring damage can be used to monitor the propagation of a crack in a damaged structure. With the use of proper comparison technology, the data could be used to determine the structural health of concrete elements. The use of thermography technology to monitor a cracked structure would enable to monitor the propagation of the crack in a structure that is exposed to high temperatures as seen in a nuclear plant, etc. The use of such technology could improve safety by early identification of structural flaws that may have otherwise been overlooked. Further research will be undertaken in the future to explore the use of FBG sensors and IR thermography in concrete structures in SHM.

## 6. References

- 1 Biswas P , Bandyopadhyaya S., Kesavanb K., Parivallal S , Arun Sundaramb , B, Ravisankar , K, Dasguptaa K ,2009 Investigation on packages of fibre Bragg grating for use as embeddable strain sensor in concrete structure
- 2 Epaarachchi, JA, Clegg, RC & Canning, J 2007, 'Investigation of the use of Near Infrared FBG (830nm) sensors for Monitoring the Structural Response of 0/90 Woven cloth/CSM Glass Fibre composite under Static and Fatigue Loading', Proceedings of Health and Usage Monitoring Systems Conference, DSTO, Melbourne.
- 3 Epaarachchi, JA, Canning, J and Stevenson, M 2009, 'The response of embedded NIR (830nm) Fibre Bragg Grating (FBG) sensors in Glass Fibre Composites under Fatigue Loading', Journal of Composite Structures.
- 4 Herszberg I, Bannister M.K, Li C.H, Thomson R.S, White C 2008, Structural health monitoring for advanced composite structures.
- 5 Hill, K.O. and Meltz, G. 1997, 'Fiber Bragg grating technology fundamentals and overview, Journal of Lightwave Technology. 15(8), 1263–1276 (1997)'
- 6 Meltz, G, Morey, WW & Glenn, WH 1989, 'Formation of Bragg gratings in optical fibres by transverse holographic method', Opt. Lett., vol.14, pp. 823 -825.
- 7 Priestley M J N 1981 'Thermal stresses in concrete bridge structures 'proceedings,'Canadian structural concrete conference Toronto' 1981, pp 255-283.  
Rosen B.W 1964, Tensile failure of fibre composites.
- 7 Kahandawa Gayan C., Epaarachchi Jayantha , Wang Hao 2011 Use of FBG sensors in SHM of Aerospace structures.
- 9 Kashyap, R, McKee, PF, Campbell, RJ & Williams, DL 1999, 'A novel method of writing photo induced chirp Bragg grating in optical fibres', Electron Lett, vol. 32, no. 17, pp. 1559-1561.
- 10 Karbhari V. M , Ansari 2009 , Structural Health Monitoring of Civil Infrastructure Systems, 1st Edition. eBook ISBN :9781845696825.
- 11 Karbhari V. M 2005, 'Sensing Issues in Civil Structural Health Monitoring 'pp 301-310.
- 12 Kersey, AD, Davis, MA, Patrick, HJ, LeBlanc M, Koo, KP, Askins, CG, Putnam, MA & Friebele, EJ 1997, 'Fibre grating sensors', Journal of Lightwave Technology, vol.15, no.8, pp. 1442–1463.
- 13 Kinet Damien, Patrice Mégret 1, Keith W. Goossen 2, Liang Qiu 3, Dirk Heider 2 and Christophe Caucheteur ,2014 'Fiber Bragg Grating Sensors toward Structural Health Monitoring in Composite Materials: Challenges and Solutions 'Sensors 2014, 14, 7394-7419; doi:10.3390/s140407394.
- 14 Takeda S, Okabe Y and Takeda N, 2008, "Monitoring of delamination growth in CFRP laminates using chirped FBG sensors", Journal of Intelligent Material Systems and Structures, vol.19, no.4, pp. 437-444.
- 15 X. W. Ye,<sup>1</sup> Y. H. Su,<sup>2</sup> and J. P. Han<sup>2</sup> . Structural 2014, Health Monitoring of Civil Infrastructure Using Optical Fiber Sensing Technology: A Comprehensive Review.